Original Articles

A small molecule targeting the interaction between human papillomavirus E7 oncoprotein and cellular phosphatase PTPN14 exerts antitumoral activity in cervical cancer cells

Chiara Bertagnin [a], Lorenzo Messa [a], Matteo Pavan [b], Marta Celegato [a], Mattia Sturlese [b], Beatrice Mercorelli [a], Stefano Moro [b], Arianna Loregian [a,*]

[a] *Department of Molecular Medicine, University of Padua, Padua, Italy*
[b] *Molecular Modeling Section (MMS), Department of Pharmaceutical and Pharmacological Sciences, University of Padua, Padua, Italy*

ARTICLE INFO

ABSTRACT

Human papillomavirus (HPV)-induced cancers still represent a major health issue for worldwide population and lack specific therapeutic regimens. Despite substantial advancements in anti-HPV vaccination, the incidence of HPV-related cancers remains high, thus there is an urgent need for specific anti-HPV drugs. The HPV E7 oncoprotein is a major driver of carcinogenesis that acts by inducing the degradation of several host factors. A target is represented by the cellular phosphatase PTPN14 and its E7-mediated degradation was shown to be crucial in HPV oncogenesis. Here, by exploiting the crystal structure of E7 bound to PTPN14, we performed an *in silico* screening of small-molecule compounds targeting the C-terminal CR3 domain of E7 involved in the interaction with PTPN14. We discovered a compound able to inhibit the E7/PTPN14 interaction *in vitro* and to rescue PTPN14 levels in cells, leading to a reduction in viability, proliferation, migration, and cancer-stem cell potential of HPV-positive cervical cancer cells. Mechanistically, as a consequence of PTPN14 rescue, treatment of cancer cells with this compound altered the Yes-associated protein (YAP) nuclear-cytoplasmic shuttling and downstream signaling. Notably, this compound was active against cervical cancer cells transformed by different high-risk (HR)-HPV genotypes indicating a potential broad-spectrum activity. Overall, our study reports the first-in-class inhibitor of E7/PTPN14 interaction and provides the proof-of-principle that pharmacological inhibition of this interaction by small-molecule compounds could be a feasible therapeutic strategy for the development of novel antitumoral drugs specific for HPV-associated cancers.

1. Introduction

Human papillomaviruses (HPVs) are small double-stranded DNA viruses with epithelial tropism and are highly prevalent human pathogens in worldwide population. Low-risk HPV genotypes mainly cause cutaneous flat warts, while high-risk HPVs (HR-HPV), such as HPV16 and HPV18, are responsible for virtually all cases (~99%) of cervical carcinoma and several other types of tumors, including anogenital and head-and-neck cancers [1,2].

Although vaccination reduced the burden of HR-HPV infections [3], cervical cancer is still the most common female malignancy in 23 countries worldwide [4]. On the other hand, no specific anti-HPV drugs exist yet in the clinics. Considering the multitude of people already infected by HR-HPV strains and at risk of developing cancer, the

numerous subjects who cannot be vaccinated, and the growing distrust for vaccines, the number of cancer cases caused by HPV infection is expected to increase in the next years [5]. Therefore, there is an urgent need for specific treatments for HPV-associated tumors.

The carcinogenic potential of HR-HPVs is linked to the major viral oncoproteins E6 and E7 [6]. E7 is a small protein without enzymatic activity that exerts its functions solely through protein-protein interactions (PPIs) with several cellular partners. These PPIs are driven by the LxCxE motif in the N-terminal domain of E7, which is intrinsically disordered, and by two surface patches with strict sequence conservation located in the C-terminal CR3 domain, the only structured region of the protein [7–9]. The binding of E7 to host factors results in the degradation of key proteins involved in cellular homeostasis, such as pRb and p21, thus promoting carcinogenesis [10–12]. Moreover, E7 can

---

modulate the activity of cellular kinases, e.g., AKT and PKM2, contributing to the malignant phenotype [13,14]. Recently, the importance of the interaction between E7 and PTPN14 and the consequent proteasomal degradation of PTPN14 were described [15]. PTPN14 is a large non-transmembrane protein tyrosine phosphatase (PTP) which possesses two central proline-rich domains (PPxY) involved in interactions with proteins containing a double-tryptophan (WW) motif [16]. One of these proteins is the transcriptional co-activator Yes-associated protein (YAP), a downstream effector of the Hippo pathway and a strong oncogenic determinant in solid tumors [17,18]. PTPN14 can interact with YAP and induce its cytoplasmic retention, thereby inhibiting its transcriptional activity [19]. Thus, since YAP nuclear accumulation and downstream signaling activation are a common feature of several types of cancers, PTPN14 likely behaves as an oncosuppressor [20,21]. The E7 proteins of several HPV genotypes are able to interact with the catalytic PTP domain of PTPN14 (hereafter called PTPN14-PTP) via the CR3 domain [15,22,23]. As a consequence of this interaction, high-risk E7 variants can trigger the proteasomal degradation of PTPN14 through the ubiquitin ligase UBR4/p600 [15,22,23] and abrogate PTPN14 oncosuppressive activity.

Recently, the crystal structure of the CR3 domain of HPV18 E7 bound to PTPN14 was solved [24]. By exploiting this structure, we performed an *in silico* screening of small-molecule libraries to search for compounds able to disrupt the E7/PTPN14 interaction and hence restore the endogenous levels of PTPN14 in cervical cancer cells. Here, we report the discovery and characterization of the first-in-class inhibitor of this PPI, capable of relieving PTPN14 from E7-mediated degradation and endowed with antitumoral properties. PTPN14 rescue, in turn, resulted in the modulation of YAP shuttling and signaling. We also show that this compound possesses activity against cervical cancer cells harboring different HR-HPV genotypes. Thus, we provide the proof-of-concept that the E7/PTPN14 interaction can be successfully blocked by a small-molecule compound, paving the way for the development of novel and specific anti-HPV therapies.

2. Materials and methods

2.1. Structure-based virtual screening

A multistage Structure-Based Virtual Screening (SBVS) derived from the experience in the D3R Grand Challenge 2 [25], was performed to identify potential binders of the CR3 domain of HPV18 E7 protein. A library of around 2 million commercially available compounds gathered from several vendors was screened taking advantage of the structural information encoded in the crystal complex (PDB ID: 6IWD) between the CR3 domain of HPV18 E7 and the PTP domain of PTPN14. The docking-based virtual screening was carried out on the HPV18 E7 interface of the protein-protein interaction through the PLANTS software [26]. The resulting docking poses were filtered based on a series of descriptors implemented in MOE 2019.01 and refined through short molecular dynamics simulations. The final compounds selection was based on pose stability, visual inspection, and chemical diversity. A full description of each screening step is available in Supplementary Data.

2.2. Compounds and peptides

Hit compounds were purchased from Enamine (compounds 1–19, 44–46), Life Chemicals (20–37), Asinex (38–39), and Otava Chemicals (40–43). Compound Cpd12 targeting HPV E6 oncoprotein [27,28] was purchased from SPECS. The anti-influenza compound 54 was previously described [29]. All compounds were dissolved in DMSO and stock solutions were stored at −20 °C. The E7 α1-peptide was purchased from ProteoGenix (France) and dissolved in DMSO. The $PB1_{1-15}$ peptide (corresponding to residues 1–15 of the PB1 subunit of influenza virus RNA polymerase) was previously reported [30].

2.3. Expression and purification of recombinant proteins

The 6His-PTPN14-PTP (residues 857–1187), $6His\text{-}HPV16\ E6_N$ (residues 1–80), and HPV16 E7 (full-length) proteins were expressed in *E. coli* and purified by different protocols that are described in detail in the Supplementary Data.

2.4. ELISA-based E7/PTPN14 interaction assay

To detect the E7/PTPN14 interaction *in vitro*, 96-well microtiter plates (Nuova Aptaca) were coated with 6His-PTPN14-PTP and incubated overnight with increasing amounts of untagged HPV16 E7, or $6His\text{-}E6_N$ as a negative control. Interactions were detected using either an anti-HPV16 E7 antibody (NM2, Santa Cruz) or an anti-HPV16 E6 antibody (N-17, Santa Cruz) followed by the incubation with a horseradish peroxidase (HRP)-conjugated secondary antibody and the chromogenic 3,3′,5,5′ tetramethylbenzidine (TMB) substrate for spectrophotometric measurements. Absorbance was read at 450 nm onto a microplate reader (MultiSkan FC, Thermo Scientific). For inhibition assays (in the presence of test compounds), microtiter plates coated with 6His-PTPN14-PTP were incubated overnight with HPV16 E7 in the presence of increasing concentrations of test compounds, or E7 α1-peptide or DMSO as controls. Binding of E7 was detected as described above.

2.5. Cell lines

HPV-positive HeLa (HPV18), CaSki (HPV16), MS751 (HPV45), ME180 (HPV68), HPV-negative C33A cervical carcinoma cells, and human foreskin fibroblasts (HFF) were purchased from American Type Culture Collection (ATCC). HaCaT (non-tumoral immortalized human skin keratinocytes) were purchased from NeoBiotech (France). All cell lines, except for CaSki and HaCaT cells, were maintained in Dulbecco modified Eagle's medium (DMEM; Life Technologies) supplemented with 10% fetal bovine serum (FBS; Life Technologies), 100 U/ml penicillin, and 100 mg/ml streptomycin sulfate (P/S; Life Technologies). CaSki were cultured in RPMI medium (Life Technologies) supplemented with 10% FBS and P/S. HaCaT were cultured in MEM medium (Gibco) supplemented with 15% FBS and P/S. Cells were kept in culture for no more than 4 weeks and were regularly tested for mycoplasma contamination.

2.6. Cell viability assay

Cell viability was determined by the 3-(4,5-dimethylthiazol-2-yl)-2,5-diphenyl tetrazolium bromide (MTT) method as previously described [27,28].

2.7. Immunofluorescence and western blotting

Immunofluorescence studies were performed as previously described [31] with minor modifications, see Supplementary Data for details. For Western blot analyses, whole cell extracts were prepared as previously described [27,32]. For full description of Western blotting procedure and a complete list of the antibodies used in this study see Supplementary Data and Table S1.

2.8. Quantitative Real-Time PCR (qPCR)

Total RNA was purified with RNA Purification Plus kit (Norgen Biotek) from HeLa cells treated for 48 h with test compounds. cDNA was generated from RNA (1.5 μg) using random primers (Applied Biosystems) and MultiScribe reverse transcriptase (Applied Biosystems). qPCR was performed with SYBR green (Applied Biosystems) on a QuantStudio 3 Real-Time PCR System (Applied Biosystems). A complete list of primer sequences can be found in Table S2.

2.9. Cell proliferation and clonogenic assays

For cell proliferation assays, HeLa, C33A, and HaCaT cells were seeded in a 96-well plate at a density of 1000 cells/well in complete medium. Twenty-four hours after seeding (day 0), cells were treated with test compounds at different concentrations for 1–4 more days. Cell proliferation was evaluated by MTT assay as described above. Clonogenic assays were performed as previously described [27]. See Supplementary Data for a more detailed method description.

2.10. Cell migration and invasion assays

Wound healing and transwell migration assays with HeLa cells were performed as previously described [28]. For transwell invasion assays, HeLa cells were treated with test compounds for 24 h and then reseeded into the upper chamber of transwell inserts (8 μm pore size; Corning) in serum- and compound-free medium. A thin layer of Matrigel (Corning) diluted 1:50 in serum-free medium was added to the membrane matrix prior to seeding. Coated inserts were placed onto a 24-well plate containing 600 μL of medium with 20% FBS as a chemoattractant. After 24 h, cells were fixed and stained and representative images of migrated cells were taken under phase-contrast microscopy. A detailed method description can be found in Supplementary Data.

2.11. Cervosphere formation assay

To evaluate the effect of the compounds on spheroid formation, HeLa cells were seeded on 24-well Nunclon Sphera plates (Thermo Fisher Scientific) at a density of 1000 cells/well, in the presence of DMSO or increasing concentrations of test compounds. Cells were cultured in Keratinocyte-SFM (Gibco) supplemented with 10 ng/ml b-FGF (Gibco), 10 ng/ml EGF (Gibco) and B27 (Gibco). Culture medium was changed every day to provide fresh compounds and tumor spheres growth was monitored daily for 10 days.

2.12. Ligand-based homology modeling

The binding mode of compound 20 on E7 protein from different HPV subtypes was modeled through the "ligand-based homology modeling" approach [33], as implemented in MOE 2019.01, using the docking pose of compound 20 on HPV18 E7 (PDB ID: 6IWD) as a template. See Supplementary Data for details.

2.13. Statistical analysis

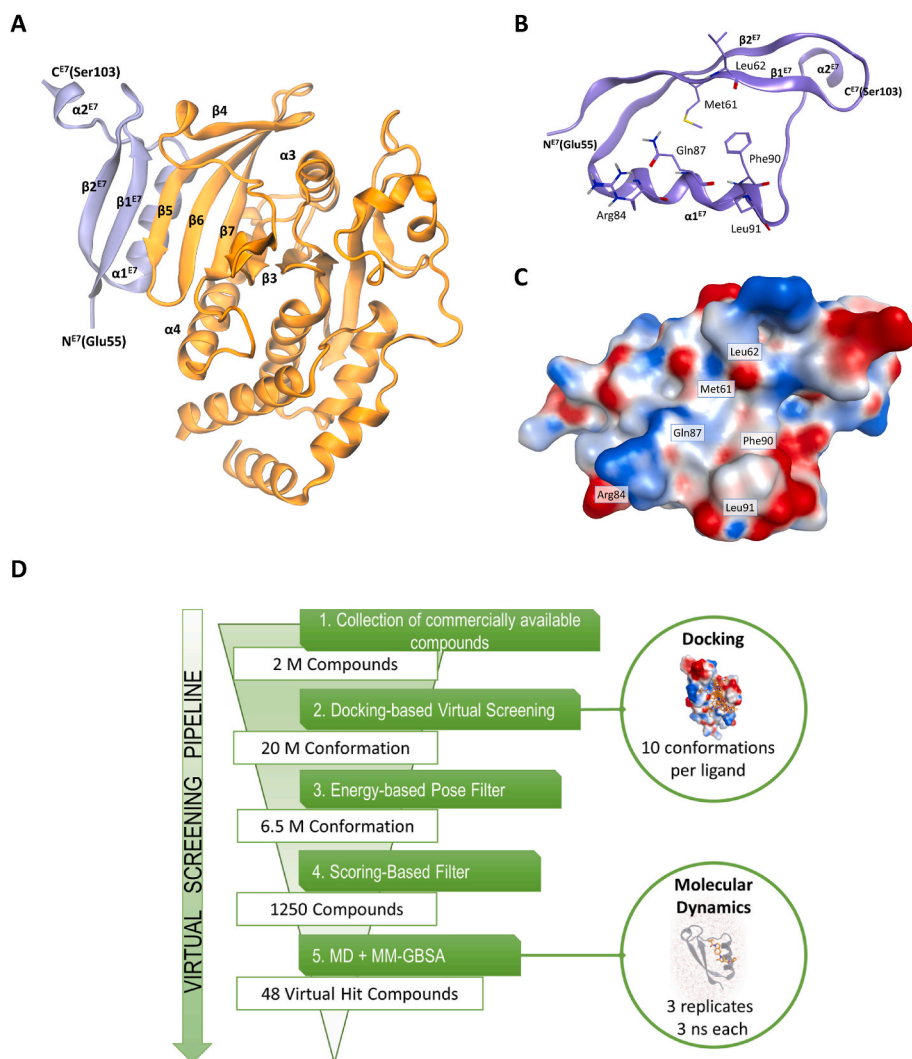Data were analyzed using GraphPad Prism 8 (GraphPad Software Inc.).

Fig. 1. Structural features of the CR3 domain of HPV18 E7 interacting with PTPN14 and virtual screening pipeline to search for E7/PTPN14 interaction inhibitors.
(A) Representation of the complex between the CR3 domain of HPV18 E7 (violet) and the PTP domain of cellular PTPN14 (orange), deposited in the Protein Data Bank with accession code 6IWD. (B) The CR3 domain of HPV18 E7 protein is represented as violet ribbon and key interacting residues with PTPN14 are shown as sticks. (C) HPV18 E7 CR3 domain is represented as a Connolly surface, with residues colored according to their electrostatic properties. Red indicates a negatively charged region, blue a positively charged one and white a neutral/uncharged one. (D) Schematic representation of the workflow adopted for the *in silico* structure-based screening of compound libraries.

3. Results

3.1. Identification of candidate inhibitors of E7/PTPN14 interaction by in silico screening

With the aim of identifying small-molecule compounds targeting the interaction of E7 with PTPN14, we performed a multistage structure-based virtual screening of ~2 million compounds belonging to different commercial libraries using the structure published by Yun and colleagues [24], in which the CR3 domain of HPV18 E7 is bound to the PTPN14-PTP domain (Fig. 1A).

Compounds were docked to the binding groove corresponding to the E7 side of the protein-protein interaction complex (Fig. 1B and C) using the PLANTS docking software: for each ligand, ten different poses were generated (Fig. 1D). Only the conformations having both a negative (therefore attractive) van der Waals and electrostatic energy were retained (6.5 M). Afterwards, 1,250 non-redundant ligand poses were selected to undergo Molecular Dynamics (MD) post-docking refinement. These included the best 250 poses according to the PLP scoring function, the best 250 according to MOE dockPki scoring function, the best 250 according to the strength of hydrogen bonds, the best 250 according to a score accounting for the hydrophobic contacts and, the best 250 according to electrostatic interaction (Fig. 1D). Finally, the poses' stability was comparatively assessed through short (3 ns) molecular dynamics simulations. Eventually, 48 virtual hit compounds were selected for biological evaluation based on pose stability, visual inspection, and chemical diversity, and 46 were purchased based on commercial availability (Tables S3 and S4).

3.2. Ability of hit compounds to block the E7/PTPN14 interaction

To test the ability of the selected hits to interfere with the physical E7/PTPN14 interaction, full-length HPV16 E7 and PTPN14-PTP (aa 857–1187) were expressed in *E. coli*, purified, and used to set up an ELISA-based assay to detect E7/PTPN14 interaction *in vitro*. Microtiter plates were coated with PTPN14-PTP and then incubated with either E7 or a truncated form of HPV16 E6 oncoprotein consisting of its N-terminal zinc-finger domain ($E6_N$) as a control. Successively, an anti-E7 or an anti-E6 antibody was added, respectively. A dose-dependent increase in absorbance was detected upon addition of increasing amounts of E7 (Fig. 2A). As expected, since no interaction between PTPN14 and E6 has been reported, no binding was observed upon $E6_N$ addition (Fig. 2A).

To test whether the assay could also detect specific inhibition of the E7/PTPN14 interaction, wells coated with PTPN14-PTP were incubated with a fixed amount of E7 and increasing amounts of PTPN14-PTP or a synthetic peptide corresponding to residues 81–93 of HPV16 E7 (E7 α1-peptide), which forms an α-helix shown to interact with PTPN14 [24]. Both PTPN14-PTP (Fig. 2B) and the E7 α1-peptide (Fig. 2C) inhibited the E7/PTPN14 interaction in a dose-dependent manner. In contrast, an unrelated α-helical peptide ($PB1_{1-15}$), previously reported to inhibit another PPI (i.e., the interaction between the PA and PB1 subunits of influenza virus RNA polymerase) [30], showed no effects on E7/PTPN14 binding (Fig. 2C).

Next, we used this assay to test the effects of the hits emerged from the screening on E7/PTPN14 interaction. In dose-response analyses, three hit compounds, i.e., 20, 23, and 28, resulted to be active in blocking the binding of E7 to PTPN14 with inhibitory concentration at half-maximal response (IC_{50}) values in the low micromolar range and similar to the IC_{50} of E7 α1-peptide (Fig. 2D and S1). Other hit compounds, i.e., 19, 22, 27, and 42, showed a dose-dependent inhibition of E7/PTPN14 binding but with higher IC_{50}s (Fig. 2D). The remaining compounds did not significantly affect the E7/PTPN14 interaction up to a concentration of 100 μM (Fig. 2D). To test the specificity of hits' activity, we also tested all the compounds in a similar ELISA-based interaction assay that can detect the inhibition of influenza virus PA/PB1 interaction [30]. None of the anti-E7/PTPN14 hits inhibited the PA/PB1
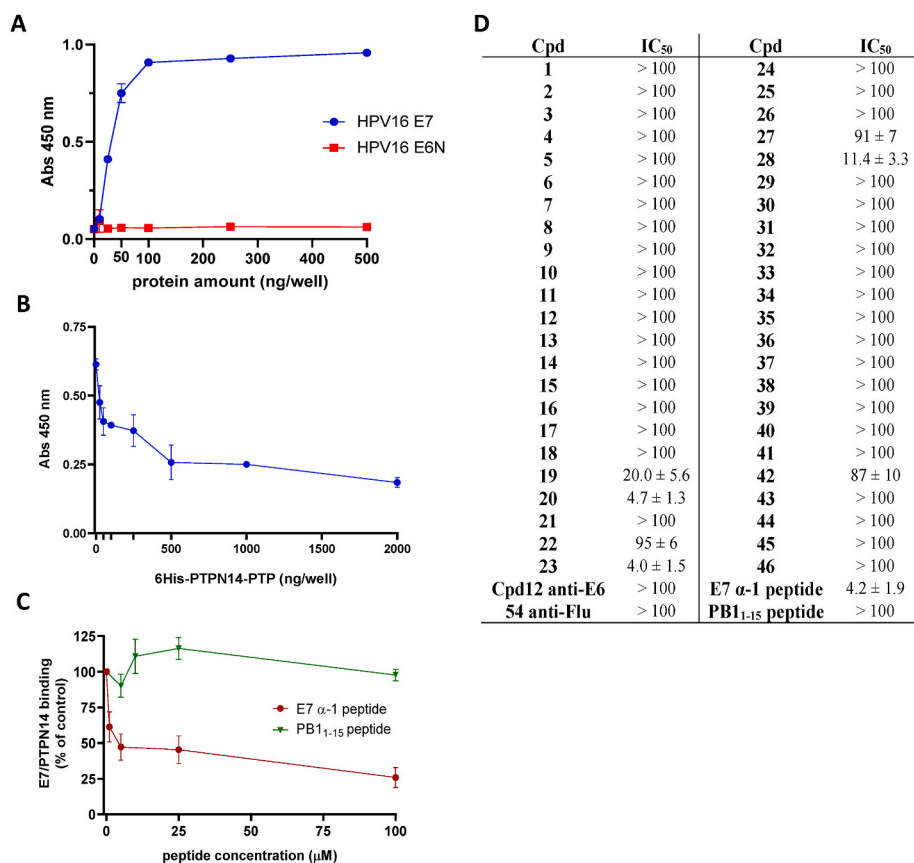
Cpd	IC_{50}	Cpd	IC_{50}
1	> 100	24	> 100
2	> 100	25	> 100
3	> 100	26	> 100
4	> 100	27	91 ± 7
5	> 100	28	11.4 ± 3.3
6	> 100	29	> 100
7	> 100	30	> 100
8	> 100	31	> 100
9	> 100	32	> 100
10	> 100	33	> 100
11	> 100	34	> 100
12	> 100	35	> 100
13	> 100	36	> 100
14	> 100	37	> 100
15	> 100	38	> 100
16	> 100	39	> 100
17	> 100	40	> 100
18	> 100	41	> 100
19	20.0 ± 5.6	42	87 ± 10
20	4.7 ± 1.3	43	> 100
21	> 100	44	> 100
22	95 ± 6	45	> 100
23	4.0 ± 1.5	46	> 100
Cpd12 anti-E6	> 100	E7 α-1 peptide	4.2 ± 1.9
54 anti-Flu	> 100	$PB1_{1-15}$ peptide	> 100

Fig. 2. Effects of hit compounds on PTPN14/E7 binding.
(A) Recombinant PTPN14-PTP domain was used to coat microtiter plates and increasing amounts of HPV16 E7, or another protein (HPV16 $E6_N$) as a control, were added. Samples were then incubated with the appropriate primary and secondary HRP-conjugated antibody and bound proteins were detected by spectrophotometric measurements at 450 nm. (B) Increasing amounts of PTPN14-PTP were added together with a fixed amount of E7 to wells coated with PTPN14-PTP. Binding of E7 was detected as described above. The absorbance at 450 nm measured in the presence of the competitor is plotted. (C) Increasing amounts of E7 α1-peptide or $PB1_{1-15}$ peptide as a negative control were added together with a fixed amount of E7 to wells coated with PTPN14-PTP. Binding of E7 was detected as described above. The percentage of the E7/PTPN14 binding measured in the presence of inhibitors with respect to that measured in the absence of inhibitors is plotted. (D) The ability of the 46 hit compounds to disrupt the E7/PTPN14 interaction was assessed by the ELISA-based E7/PTPN14 interaction assay. The inhibitory concentration at half-maximal response (IC_{50}) values are reported. The E7 α1-peptide was used as a positive control, while the anti-HPV E6 compound Cpd12, the anti-influenza compound 54 and $PB1_{1-15}$ peptide were used as negative controls. In all panels, data shown represent the mean ± SD of three independent experiments.

interaction up to a concentration of 100 μM (data not shown). As a further specificity control, we tested against E7/PTPN14 interaction two compounds previously reported to inhibit other PPIs, i.e., Cpd12, which blocks the interaction between HPV E6 and the cellular oncosuppressor p53 [27,28], and compound 54, which interferes with influenza virus PA-PB1 interactions [29,34]. Both Cpd12 and 54 did not exhibit any inhibitory activity on E7/PTPN14 binding (Fig. 2D and S1).

Thus, these results indicated that some hit compounds selected from the virtual screening can inhibit specifically and in a dose-dependent manner the interaction between E7 and PTPN14-PTP. The low hit rate most likely is due to the difficulties in targeting PTPN14/E7 interface, which consists of a flat surface. It should be considered that the fraction of the accessible surface area (% rSASA) of compound 20 exposed to the solvent is around 44%, which is an extremely high value if compared to those of other ligands complexed in the already solved ligand-protein structures also among other PPI inhibitors [35].

3.3. Cytotoxic activity of hit compounds against HPV-positive cervical cancer cells

In parallel to the ELISA experiments, we also tested the cytotoxic activity of all hit compounds by MTT assays in two HPV-positive cervical cancer cell lines, i.e., HeLa (HPV18) and CaSki (HPV16), and for comparison in HPV-negative C33A cervical cancer cells and non-tumoral keratinocytes and fibroblasts, i.e., HaCaT and HFF cells. Several of the compounds showed no cytotoxic activity against any of the tested cell lines, including some of the molecules that showed inhibitory activity on the E7/PTPN14 interaction, i.e. compounds 19 and 42 (Table 1 and Fig. 2D). On the other hand, treatment with some hits (i.e., compounds 4, 11, 15, 17, 22, 27, 29, 30, 31, 32, 35, 39, 41, 44, and 46) affected the viability of HeLa and/or CaSki cells, but also resulted in non-specific cytotoxic activity against HPV-negative C33A cells (Table 1). Importantly, the most active E7/PTPN14 inhibitors – compounds 20, 23, and 28 – remarkably affected the viability of both HPV-positive cancer cell lines (with IC$_{50}$s 15.2 ± 5.8 μM, 14.0 ± 3.5 μM, and 1.40 ± 0.02 μM in HeLa cells, respectively; 6.6 ± 0.7 μM, 9.0 ± 1.9 μM and 5.5 ± 0.4 μM in CaSki cells, respectively), without showing toxicity (IC$_{50}$ > 250 μM) against either HPV-negative C33A cancer cells or non-tumoral cells (Table 1). Thus, three small molecules that block the E7/PTPN14 interaction also selectively affect the viability of HPV-positive cervical cancer cells.

3.4. Compound 20 increases PTPN14 levels and induces the cytoplasmic relocalization and transcriptional inactivation of YAP in HPV-positive cells

Since the physical interaction between E7 and PTPN14 results in E7-mediated proteasomal degradation of the cellular phosphatase, we next investigated whether the treatment with the most active hit compounds (i.e., 20, 23, and 28) was able to increase PTPN14 levels in HPV-positive cells. In these experiments, a siRNA targeting *E6/E7* expression and an inactive hit (compound 33) were used as a positive and a negative control, respectively. As expected, *E6/E7* silencing led to a very high increase of PTPN14 levels due to the simultaneous downregulation of both oncogenes and thus to the inhibition of both E7-mediated degradation of PTPN14 and E6-mediated degradation of p53. In fact, E6 oncoprotein is known to degrade p53 [36], which also drives *PTPN14* gene transcription [37]. In HeLa cells compound 20 showed the ability to restore PTPN14 levels in a concentration-dependent manner, as detected by both immunofluorescence and Western blot (Fig. 3A, B, S2A, and S2B). In contrast, treatment with compounds 23 and 28, as well as with the inactive compound 33, did not increase PTPN14 levels (Fig. 3A and B). A possible explanation for the latter result could be that differently from the ELISA (where only E7 and PTPN14 proteins are present), in the cellular context other, known or yet unknown, E7 cellular binding partners which like PTPN14, bind within or in proximity of the CR3 region of E7 might be involved, thus interfering with PTPN14 rescue by

Table 1

Effects of hit compounds on the viability of HPV-positive and HPV-negative cells.

Compound	Cytotoxic activity, IC$_{50}$ (μM)				
	HeLa	CaSki	C33A	HaCaT	HFF
1	>250	>250	>250	n.d.	n.d.
2	>250	>250	>250	n.d.	n.d.
3	>250	>250	>250	n.d.	n.d.
4	215 ± 7	203 ± 18	205 ± 14	n.d.	n.d.
5	>250	>250	>250	n.d.	n.d.
6	>250	>250	>250	n.d.	n.d.
7	>250	>250	>250	n.d.	n.d.
8	190 ± 12	>250	>250	n.d.	n.d.
9	230 ± 15	>250	>250	n.d.	n.d.
10	>250	>250	250	n.d.	n.d.
11	92 ± 20	125 ± 9	43 ± 4	n.d.	n.d.
12	>250	>250	>250	n.d.	n.d.
13	>250	>250	>250	n.d.	n.d.
14	>250	>250	>250	n.d.	n.d.
15	106 ± 27	>250	45 ± 11	n.d.	n.d.
16	>250	>250	>250	n.d.	n.d.
17	128 ± 4	248 ± 1	108 ± 11	n.d.	n.d.
18	>250	>250	>250	n.d.	n.d.
19	>250	>250	>250	n.d.	n.d.
20	$\mathbf{15.2 \pm 5.8}$	$\mathbf{6.6 \pm 0.7}$	**> 250**	**> 250**	**> 250**
21	>250	>250	>250	n.d.	n.d.
22	57 ± 5	102 ± 10	69 ± 6	n.d.	n.d.
23	$\mathbf{14.0 \pm 3.5}$	$\mathbf{9.0 \pm 1.9}$	**> 250**	**> 250**	**> 250**
24	>250	>250	>250	n.d.	n.d.
25	>250	>250	>250	n.d.	n.d.
26	>250	>250	>250	n.d.	n.d.
27	209 ± 12	>250	189 ± 1	n.d.	n.d.
28	$\mathbf{1.40 \pm 0.02}$	$\mathbf{5.5 \pm 0.4}$	**> 250**	**> 250**	**> 250**
29	220 ± 14	235 ± 19	208 ± 11	n.d.	n.d.
30	81 ± 6	185 ± 35	19 ± 5	n.d.	n.d.
31	183 ± 24	>250	31 ± 1	n.d.	n.d.
32	8 ± 2	125 ± 12	95 ± 8	n.d.	n.d.
33	>250	>250	>250	n.d.	n.d.
34	>250	>250	>250	n.d.	n.d.
35	105 ± 13	112 ± 7	105 ± 8	n.d.	n.d.
36	>250	>250	>250	n.d.	n.d.
37	>250	>250	>250	n.d.	n.d.
38	>250	>250	>250	n.d.	n.d.
39	174 ± 28	236 ± 1	174 ± 6	n.d.	n.d.
40	>250	>250	>250	n.d.	n.d.
41	>250	>250	58 ± 7	n.d.	n.d.
42	>250	>250	>250	n.d.	n.d.
43	>250	>250	>250	n.d.	n.d.
44	>250	>250	230 ± 28	n.d.	n.d.
45	127 ± 2	>250	>250	n.d.	n.d.
46	209 ± 15	244 ± 5	86 ± 13	n.d.	n.d.

Cell viability of compound-treated HeLa (HPV18) and CaSki (HPV16) cells was assessed by MTT assay at 48 h post-treatment. HPV-negative C33A cervical cancer cells and non-tumoral cells (HaCaT and HFF) were used as specificity controls. The IC$_{50}$ values (compound concentration that inhibits 50% cell viability) are reported. Data represent the mean $\pm$ SD of three independent experiments in duplicate.

compounds 23 and 28. In line with this hypothesis, when we analyzed possible effects of compounds 20, 23, and 28 on both p53 and pRb levels, we found that while none of the three compounds affected p53 levels, the treatment with compound 28 - but not with compounds 20 and 23 - appeared to increase the pRB levels (data not shown), suggesting that in the cellular context compound 28 might interfere with the E7/pRb interaction rather than the E7/PTPN14 binding. This might be explained by previous observations that in addition to the LxCxE motif of Conserved Region 2 (CR2) of E7, also the CR3 domain is involved in the interaction with pRB [11,38]. Although the activity of compound 28, and possibly also 23, warrants future investigations, they were discarded for the scope of this study.

Next, since it is known that PTPN14, by interacting with YAP, retains it in the cytoplasm, we investigated whether the rescue of the cellular phosphatase observed upon treatment with compound 20 was coupled
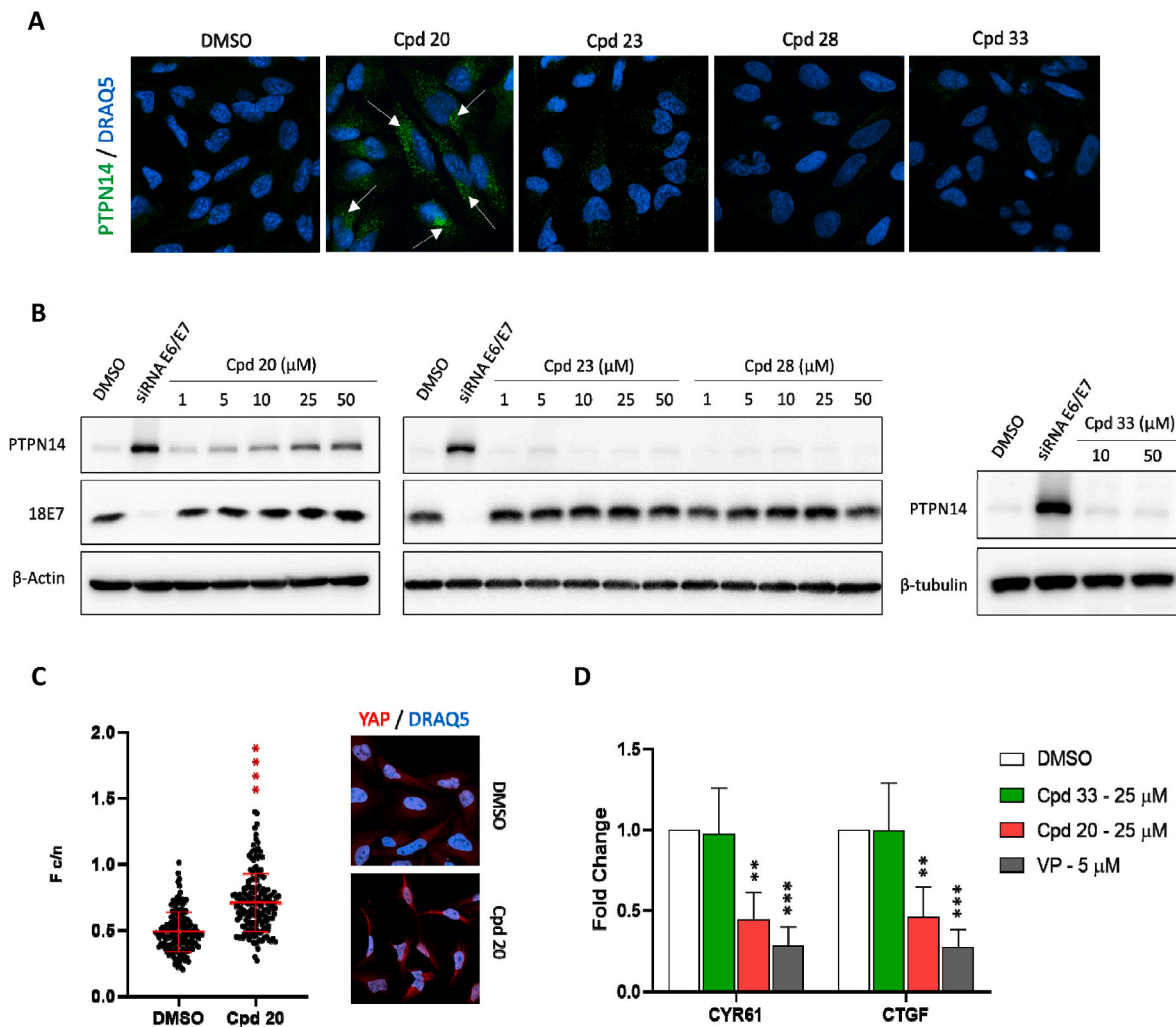
Fig. 3. Effects of selected compounds on PTPN14 levels and YAP localization and signaling.
(A) Compound 20 rescues endogenous PTPN14 protein levels. HPV18-positive HeLa cells were treated with compounds 20, 23, 28, and 33 (25 μM) for 48 h. DMSO-treated cells were included as a negative control. Cells were analyzed by immunofluorescence using a specific anti-PTPN14 primary antibody (left panels). Nuclei were stained with DRAQ5. Arrows indicate cytoplasmic PTPN14 rescue following treatment with compound 20. See Supplementary Data, Fig. S2A for scatter dot plot analysis and quantification of PTPN14 levels. (B) Compound 20 rescues PTPN14 protein levels in a concentration-dependent manner. HPV18-positive HeLa cells were treated with increasing concentrations of compounds 20, 23, 28, and 33. DMSO-treated cells were included as a negative control, along with cells in which *E6/E7* oncogenes were silenced as a positive control (siRNA E6/E7). At 72 h post-treatment, cells were harvested, lysed, and cellular lysates were analyzed by Western blotting using specific anti-PTPN14 and anti-E7 primary antibodies. β-Actin or β-tubulin were used as a loading control. Final images included in this work are representative of multiple experimental replicates. See Supplementary Data, Fig. S2B for the quantification of PTPN14 protein bands in compound 20-treated samples *versus* vehicle-treated samples. (C) Quantitative analysis of YAP intracellular localization upon compound 20 treatment. The cytoplasmic/nuclear fluorescence (Fc/n) ratio was calculated for HeLa cells treated for 48 h with compound 20 or DMSO as a control. Data are presented as scatter-dot-plots of $n_{DMSO} = 167$ cells and $n_{Cpd20} = 173$ cells. Data were analyzed by one-way ANOVA followed by Dunnett's multiple-comparisons test. ****$p < 0.0001$ compared to control (DMSO-treated cells). Right panels show representative examples of the images used for quantitative analysis. (D) The effects of test compounds (compounds 20, 33, and the positive control Verteporfin, VP) on the transcription of YAP target genes *CYR61* and *CTGF* were assessed in HeLa cells treated for 48 h by qPCR. Bar graphs represent gene transcription downregulation upon compound treatment, expressed as fold change. Data represent the mean ± SD of three independent experiments. Data were analyzed by a two-way ANOVA followed by Tukey's multiple comparison test. **$p < 0.01$; ***$p < 0.001$ compared to control (DMSO-treated cells).

to the relocalization of YAP in the cell cytoplasm. We thus performed quantitative single-cell immunofluorescence analysis of YAP localization in HeLa cells treated with the small molecule. Strikingly, we observed that the average nuclear accumulation of YAP in treated cells was significantly lower than that in untreated control cells (Fig. 3C), indicating that compound 20-mediated PTPN14 rescue could induce YAP shuttling towards the cytoplasmic compartment.

Therefore, we investigated the effect of compound treatment on the transcription of genes related to YAP signaling cascade. Consistently with the above data, compound 20 was able to downregulate endogenous mRNA levels of *CYR61* and *CTGF*, two bona fide YAP target genes [17], in HeLa cells (Fig. 3D). Verteporfin, a known inhibitor of the

YAP/TEAD interaction [39,40], was used as a positive control. In contrast, treatment with compound 33 had no effect (Fig. 3D).

Altogether, these results indicated that in HPV-positive cervical cancer cells, compound 20, by inhibiting the E7/PTPN14 interaction and hence preventing the E7-mediated proteasomal degradation of PTPN14, could rescue PTPN14 levels. This event, in turn, was able to modulate YAP intracellular localization, promoting its shuttling toward the cytoplasm and leading to the downregulation of YAP target genes.

3.5. Compound 20 affects the proliferation, clonogenicity, migration/invasion capacity, and stem-cell survival of HPV-positive cancer cells

The inhibition of the interaction between E7 and PTPN14 was shown to cause a decrease in the proliferation capacity of HPV-positive cancer cells as a consequence of YAP-related signaling modulation [24]. Therefore, we tested the effects of compound 20 on the proliferation of HPV-positive (HeLa), or HPV-negative (C33A) and non-tumoral cells (HaCaT) for comparison. Cells were treated for 4 days with compound 20 or the inactive hit compound 33 as a negative control, and their growth compared to that of DMSO-treated cells. As shown in Fig. 4A, in short-term proliferation assays, compound 20 selectively reduced the proliferation of HeLa cells in a concentration-dependent manner, but not that of C33A and HaCaT cells, while compound 33 had no significant effect as compared to vehicle-treated cells. In a long-term clonogenic assay, the number of HeLa colonies was decreased upon treatment with compound 20 compared to those in control vehicle- or compound 33-treated cells (Fig. 4B and S3A). In contrast, no difference in colony formation was observed between untreated and compound-treated HPV-negative C33A cells (Fig. 4B and S3A).

Subsequently, we examined the effects of compound 20 on the migration and invasion capacity of HPV-transformed cells, as previous studies showed that expression in HeLa cells of mutant E7 and PTPN14 proteins defective in binding to each other led to a considerable suppression of cell motility and invasiveness [24]. We thus performed wound healing and transwell migration/invasion assays with HeLa cells treated with compound 20 or compound 33 and DMSO as controls. In wound healing assays, compound 20 significantly reduced the migration rate of HeLa cells, whereas this effect was not observed in DMSO- and compound 33-treated cells (Fig. 4C and S3B). Consistently, also in transwell assays we could observe a remarkable suppression of migration and invasion of cells treated with compound 20, but not upon treatment with DMSO or compound 33 (Fig. 4D, E, and S3C).

Finally, considering the critical role of YAP in determining stem-like potential in solid tumors [41,42], we wished to investigate whether compound 20 could also affect the survival and growth of the stem cell population of HPV-positive cervical cancer cells. Importantly, cancer stem cells represent the niche of cancer cells that drive drug resistance and are responsible for tumor relapses after drug treatment [43]. To assess this, we cultured HeLa cells in low-adhesion conditions and monitored for 10 days the growth of 3D cervospheres from single-cell suspensions in the presence of compound 20 or compound 33 and DMSO as controls. Compound 20 remarkably reduced the generation of HeLa-derived tumor spheroids as compared to compound 33-treated and DMSO-treated cells, affecting the sphere-forming efficiency (SFE) in a concentration-dependent manner (Fig. 4F and S3D). Thus, compound 20 also proved able to block the growth of 3D spheroids from cancer stem cells.

Overall, our results demonstrated that treatment with compound 20 affects the proliferation, migration capacity, and invasiveness of HPV-positive cervical cancer cells. Moreover, treatment with compound 20 reduced the stemness potential of HPV-positive cells.

3.6. Compound 20 is active against different high-risk HPV genotypes

By aligning the canonical sequences corresponding to the CR3 domain of E7 of the most prevalent mucosal HR-HPV genotypes, we noticed that the residues reported to be involved in E7/PTPN14 binding [22,24] are highly conserved among these strains (Fig. 5A). Thus, one might speculate that a dissociative inhibitor targeting these amino acids could likely have a broad-spectrum activity. Prompted by these observations, we tested compound 20 also in other commercially available HPV-positive cervical cancer cell lines, i.e., MS751 and ME180, which harbor HPV45 and HPV68, respectively. We first investigated the effects of compound 20 on the viability of these cancer cells by MTT assays. As shown in Fig. 5B, compound 20 retained its activity also in MS751 and

ME180 cells (IC_{50}s 14.3 $\pm$ 4.6 μM and 15.5 $\pm$ 3.6 μM, respectively). Next, we tested whether compound 20 was also able to restore PTPN14 levels in a panel of cervical cancer cells other than HeLa. Remarkably, we observed the rescue of PTPN14 levels in CaSki (HPV16), MS751 (HPV45), and ME180 (HPV68) cells (Fig. 5C). These results indicated that compound 20 is active against cervical cancer cells harboring different HR-HPV genotypes, thus exhibiting a potential broad-spectrum activity.

To confirm these observations at a molecular level, first the docking pose of compound 20 was deeply investigated by MD simulation to monitor the role of the key interactions established with the CR3 domain of HPV18 E7. The complex conformation obtained from the docking-based VS was used as starting point for three classical MD simulations of 100 ns each. Interestingly, the network of hydrogen bonds anchoring compound 20 to HPV18 E7 with the backbone of Thr60, Leu62, and the side chain of Gln87 resulted stable along the trajectory (Fig. S4). The hydrophobic contacts established by compound 20 with His59, Met61, Leu83, and Phe90 also played a fundamental role in stabilizing the interaction (Fig. 5D). We also repeated the MMGBSA calculation on the extended trajectories confirming the scoring obtained in the VS pipeline. In particular, the MMGBSA averaged value (ΔG_{AVG}) in the three replicates of 100 ns each was −34.53 kcal/mol, while during the three replicates of 3 ns length achieved a ΔG_{AVG} of −32.8 kcal/mol.

To simulate the interaction of compound 20 with E7 of other HR-HPV genotypes, we investigated the intermolecular interactions between compound 20 and CR3 domain of the E7 proteins of HPV16, HPV45, and HPV68. Starting from the binding mode of compound 20 on HPV18 E7, a binding hypothesis for compound 20 on each other E7 genotypic variant was obtained by ligand-based homology modeling (Fig. 5D). Interestingly, the only amino acid side chain predicted to form a direct H-bond interaction with compound 20 was Gln87 of HPV18 E7. This residue is conserved in all genotypic variants, except for HPV16 in which a Glutamic acid is present (Fig. 5A). However, the presence of a flexible arginine (Arg77) in its proximity restores the formation of the H-bond within the same ligand portion (Fig. 5D). The conservation of the defined fold of the E7 CR3 domain among different HR-HPV genotypes suggests that the predicted binding mode of compound 20 would not be perturbed by the other changes in the side chain of pocket residues in the different genotypes, confirming the results obtained in the different tested HPV-positive cell lines and heralding the prospect of a potential broad-spectrum anti-HPV activity of this compound.

4. Discussion

In this study, we explored the targeting of the interaction between the oncoprotein E7 of HR-HPV strains with the cellular phosphatase PTPN14 as a novel strategy for the development of anticancer drugs. We indeed provide the proof-of-principle that blocking the E7/PTPN14 interaction by means of small-molecule compounds is feasible and report the discovery of the first-in-class inhibitor capable of preventing E7 binding to PTPN14 and consequently E7-mediated PTPN14 degradation. Since HPV infections are still remarkably impacting on the burden of epithelial cancers worldwide [4], targeted anti-HPV therapies are highly needed [44].

HR-HPV E7 is known to possess strong oncogenic potential as a consequence of host factor deregulation required to promote viral replication, among which pRb targeting is the most well characterized event [11,12]. Indeed, E7 has been shown to be essential for cancer onset [45,46], and in settings of high transgenic expression it can be sufficient to induce malignant tumors in mice [47–49]. However, despite the importance in HPV-induced oncogenesis, anti-E7 drug discovery campaigns are almost missing. This might be explained by the poor "druggability" of the protein, being devoid of enzymatic activity, and by the intrinsically disordered nature of the N-terminal region of E7 through which the viral protein binds pRb, p21, and likely other factors required for transformation [7,50]. The latter feature hampers the
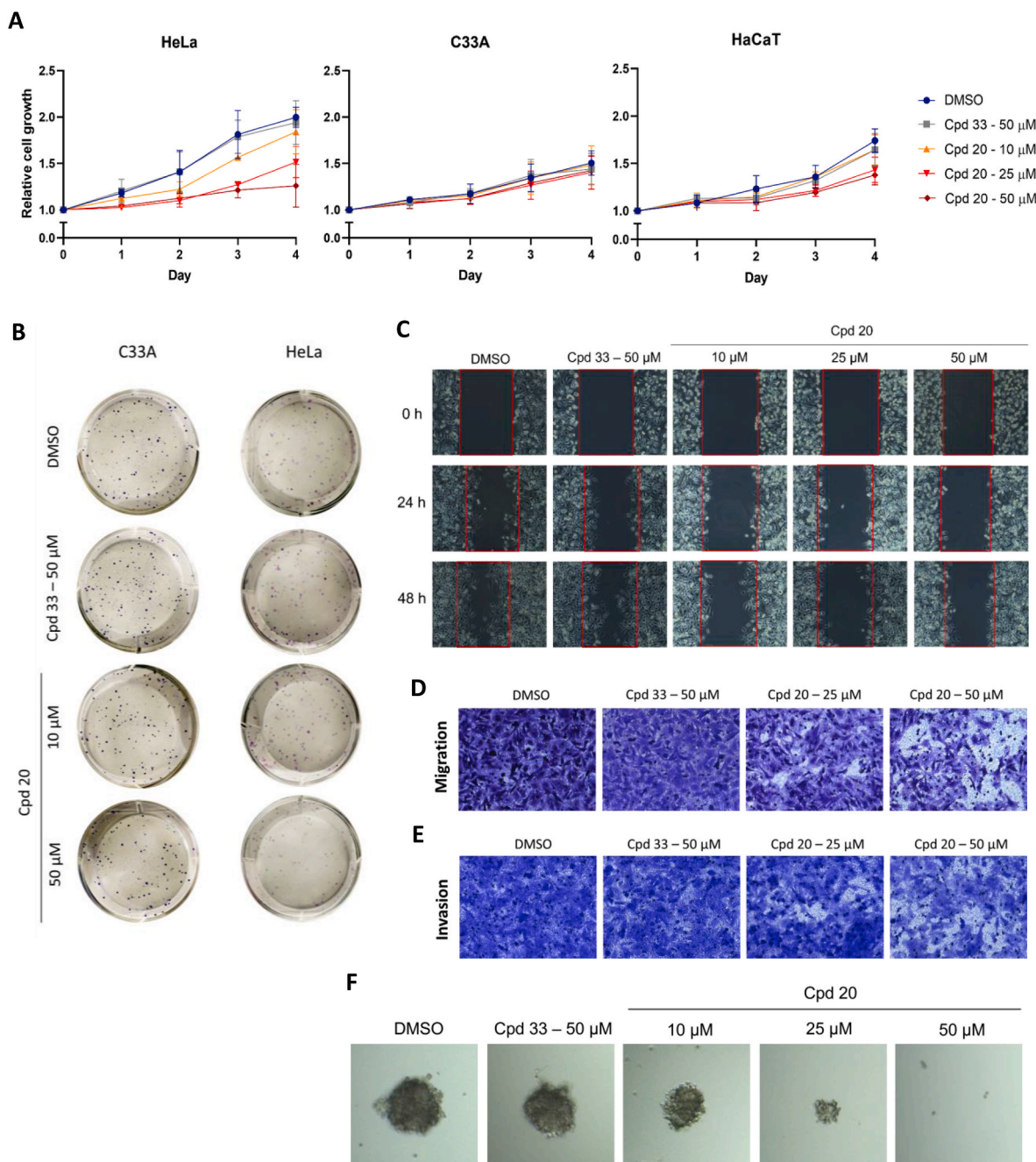
Fig. 4. Effects of compound 20 on proliferation, clonogenicity, migration/invasion capacity and stem-cell survival of HPV-positive cancer cells.
(A) Short-term proliferation assay. Growth curves of HeLa, C33A, and HaCaT cells treated with increasing concentrations of compound 20 (10, 25, and 50 μM), compound 33 as a negative control (50 μM), or DMSO were compared from day 0 to day 4. (B) Clonogenic assay with HeLa and C33A cells treated with compound 20 (10 and 50 μM), compound 33 (50 μM), or DMSO and grown for 14 days. Representative images after staining with crystal violet are shown. (C) Wound healing assay. Confluent monolayers of HeLa cells were scraped and then treated with increasing concentrations of compound 20 (10, 25, and 50 μM), or DMSO in low-serum medium. Wound closure was monitored before treatment and after 24 and 48 h, and representative images were taken using a bright-field inverted microscope (100 × magnification). (D) Transwell migration assay. HeLa cells were treated with different concentrations of compound 20 (25 and 50 μM), compound 33 (50 μM), or DMSO for 24 h. Cell migration was evaluated by transwell assays after an incubation of other 24 h in compound-free medium. Migrated cells were fixed and stained with crystal violet and representative images were taken using a bright-field inverted microscope (100 × magnification). (E) Transwell invasion assay. HeLa cells were treated as described for panel D. Transwell inserts were coated with a thin layer of Matrigel prior to cell seeding. Cell invasion was evaluated by transwell assay after an incubation of other 24 h in compound-free medium. (F) Cervospheres formation assay. The effects of test compounds on the formation of 3D tumor spheroids were evaluated by culturing HeLa cells from single-cell suspensions and monitoring the growth of cervospheres. Representative images were taken at 10 days post-seeding using a bright-field inverted microscope (100 × magnification). Compound 33 and DMSO were employed as negative controls.
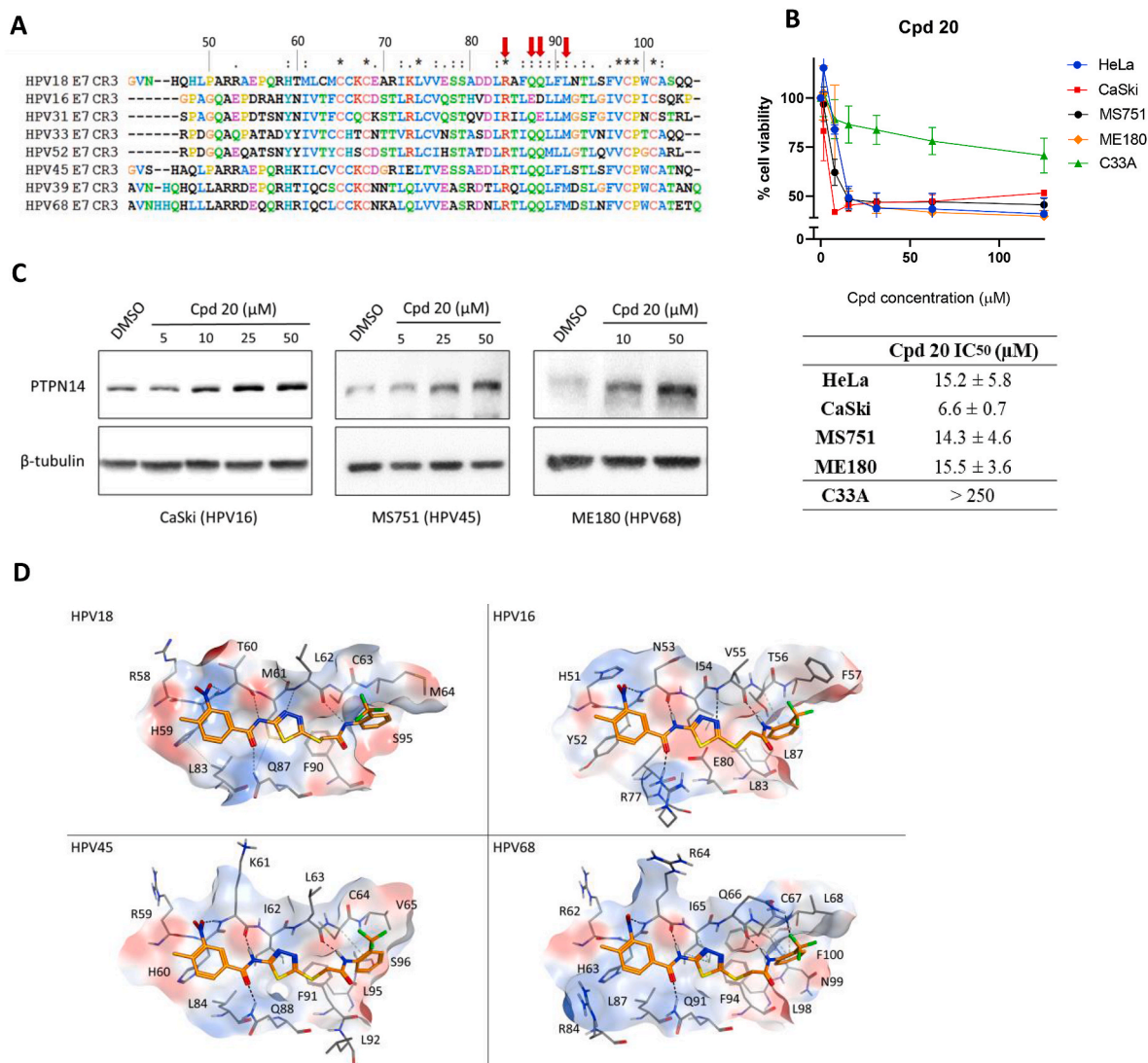
Fig. 5. Compound 20 is active against different HR-HPV genotypes.
(A) Alignment of the C-terminal amino acids of high-risk HPV E7 protein sequences. Red arrows indicate conserved E7 residues crucial for the binding to PTPN14. Top numbering refers to HPV18 E7 sequence. The symbols indicate the residue conservation according to the color-coded structural similarity of the amino acids. ".", weak conservation; ":", strong conservation; "*", full conservation. Alignment generated with ClustalX. (B) The effects of compound 20 on the viability of HPV-positive MS751 (HPV45) and ME180 (HPV68) cells were tested by MTT assay after 48 h of treatment. Data on HeLa (HPV18), CaSki (HPV16), and C33A (HPV-negative) are also shown for comparison. IC$_{50}$s represent the concentrations causing a decrease of 50% in cell viability. Data are the means ± SD derived from at least three independent experiments in duplicate. (C) Western blot analysis of PTPN14 levels in HPV-positive CaSki (HPV16), MS751 (HPV45), and ME180 (HPV68) cells upon treatment with different concentrations of compound 20. β-tubulin was used as a loading control. (D) Predicted binding mode of compound 20 with the CR3 domain of E7 from different HR-HPV genotypes: upper-left, docking pose of compound 20 on HPV18 E7 (PDB ID: 6IWD); upper-right, ligand-based homology model of compound 20 on HPV16 E7; lower-left, ligand-based homology model of compound 20 on HPV45 E7; lower-right, ligand-based homology model of compound 20 on HPV68 E7. Hydrogen bonds are depicted as dashed lines. Protein electrostatic properties are represented in either red (negatively charged) or blue (positively charged).

possibility to perform structure-based virtual screenings or to model molecules directed against that interacting module of E7.

Recent studies highlighted the importance of the interaction of E7 with PTPN14, which involves the folded CR3 domain of E7, for the pathogenesis of HPV [22,23,51]. Here, we show that disruption of this protein-protein interaction with a small-molecule inhibitor, i.e., compound 20, resulted in a rescue of cellular PTPN14 levels (Fig. 3A and B) and could counteract the malignant behavior of cervical cancer cells. In fact, compound 20-mediated rescue of PTPN14 affected YAP shuttling and downstream signaling in HPV-transformed cells (Fig. 3C and D), leading to inhibition of proliferation and migratory capacities, as well as of stemness potential (Fig. 4), which are all well-established biological phenomena activated by YAP in solid tumors [52–54]. Accordingly,

treatment with compound 20 caused the downregulation of *CYR61* and *CTGF* gene expression, two canonical YAP-target genes (Fig. 3D), in agreement with previous reports showing their downregulation in the presence of a mutated form of PTPN14 resistant to the E7-mediated degradation [24].

An important aspect is also that E7/PTPN14 binding involves residues on the CR3 domain of E7 that are highly conserved among mucosal high-risk genotypes, indicating that a dissociative inhibitor targeting this PPI might have a broad-spectrum potential. Indeed, we employed four different cervical cancer cell lines transformed by different HR-HPV genotypes (namely 16, 18, 45, and 68) and observed PTPN14 rescue upon treatment with compound 20 in all cell lines (Fig. 5). Therefore, targeting the E7/PTPN14 PPI emerges as a feasible therapeutic approach

for the development of anticancer drugs directed against a broad range of HPV-induced cancers.

The identification of compound 20 not only represents the discovery of the first-in-class E7/PTPN14 dissociative inhibitor, but also of the first small-molecule compound directly targeting the oncoprotein E7. To date, only a few studies regarding the identification of anti-E7 small molecules were reported [55,56]. Fera and colleagues targeted the E7/pRb interaction but, although they could identify a series of anti-E7/pRb inhibitors [55], those compounds were shown to bind the B domain of pRb rather than the viral protein, implying possible side-effects on pRb-mediated cellular pathways. Conversely, the strategy employed here for the identification of anti-E7/PTPN14 inhibitors was focused on searching small molecules binding directly the CR3 domain of E7, thus reducing the risk of compound-mediated effects on PTPN14 that may alter the cellular homeostasis of uninfected, non-tumoral cells. To note, Aarthy and Singh described a computational approach for the identification of anti-E7/PTPN14 inhibitors through molecular modeling predictions [56]. However, despite an extensive *in silico* characterization, none of the identified hits were tested for their biological activity in *vitro* or cell-based assays and no antitumoral effect of the candidate inhibitors was reported [56]. In contrast, here we provide evidence that compound 20 can dissociate the E7/PTPN14 protein complex and shows specific activity against HPV-transformed cells.

Overall, our study provides a significant advance in the development of much awaited targeted anti-HPV therapies. In fact, compound 20 represents a new chemical scaffold that could be used for hit-to-lead optimization and hence could be a starting point for the development of novel and specific anti-HPV drugs. The identification of another dissociative small molecule that is able to function as anticancer agent by inhibiting a PPI relevant in tumorigenesis further confirms that this therapeutic approach deserves further investigation and could provide new candidate drugs for "undruggable" targets, as in the case of Venetoclax, the first PPI inhibitor approved to treat some forms of aggressive leukemias [57]. In addition, our compound 20 could also be the starting point for potent E7 inhibitors exploiting the emerging PROteolytic TArgeting Chimeras (PROTACs) technology [58–60] and acting by inducing E7 degradation besides its inhibition, thus blocking all E7-related functions.

Funding

CRediT authorship contribution statement

Chiara Bertagnin: Writing – review & editing, Writing – original draft, Validation, Methodology, Investigation, Formal analysis, Data curation, Conceptualization. **Lorenzo Messa:** Writing – review & editing, Supervision, Methodology, Investigation, Data curation, Conceptualization. **Matteo Pavan:** Writing – review & editing, Visualization, Validation, Software, Methodology, Investigation, Formal analysis, Data curation. **Marta Celegato:** Validation, Methodology, Formal analysis, Data curation. **Mattia Sturlese:** Writing – review & editing, Writing – original draft, Software, Methodology, Investigation, Data curation, Conceptualization. **Beatrice Mercorelli:** Writing – review & editing, Writing – original draft, Supervision, Funding acquisition. **Stefano Moro:** Supervision, Software, Conceptualization, Writing – review & editing. **Arianna Loregian:** Writing – review & editing, Writing – original draft, Supervision, Investigation, Funding acquisition, Data curation, Conceptualization.

Declaration of competing interest

The authors declare that they have no known competing financial interests or personal relationships that could have appeared to influence the work reported in this paper.

Acknowledgements

Appendix A. Supplementary data

Supplementary data to this article can be found online at https://doi.org/10.1016/j.canlet.2023.216331.

References

[1] H.A. Cubie, Diseases associated with human papillomavirus infection, Virology 445 (2013) 21–34, https://doi.org/10.1016/j.virol.2013.06.007.

[2] M. Tommasino, The human papillomavirus family and its role in carcinogenesis, Semin. Cancer Biol. 26 (2014) 13–21, https://doi.org/10.1016/j.semcancer.2013.11.002.

[3] L.E. Markowitz, S. Hariri, C. Lin, E.F. Dunne, M. Steinau, G. McQuillan, E.R. Unger, Reduction in human papillomavirus (HPV) prevalence among young women following HPV vaccine introduction in the United States, National Health and Nutrition Examination Surveys, 2003-2010, J. Infect. Dis. 208 (2013) 385–393, https://doi.org/10.1093/infdis/jit192.

[4] H. Sung, J. Ferlay, R.L. Siegel, M. Laversanne, I. Soerjomataram, A. Jemal, F. Bray, Global cancer statistics 2020: GLOBOCAN estimates of incidence and mortality worldwide for 36 cancers in 185 countries, Ca - Cancer J. Clin. 71 (2021) 209–249, https://doi.org/10.3322/caac.21660.

[5] H. Damgacioglu, K. Sonawane, J. Chhatwal, D.R. Lairson, G.M. Clifford, A. R. Giuliano, A.A. Deshmukh, Long-term impact of HPV vaccination and COVID-19 pandemic on oropharyngeal cancer incidence and burden among men in the USA: a modeling study, Lancet Reg Health Am 8 (2022), 100143, https://doi.org/10.1016/j.lana.2021.100143.

[6] J. Doorbar, W. Quint, L. Banks, I.G. Bravo, M. Stoler, T.R. Broker, M.A. Stanley, The biology and life-cycle of human papillomaviruses, Vaccine 30 (Suppl 5) (2012) F55–F70, https://doi.org/10.1016/j.vaccine.2012.06.083.

[7] M.M. García-Alai, L.G. Alonso, G. de Prat-Gay, The N-terminal module of HPV16 E7 is an intrinsically disordered domain that confers conformational and recognition plasticity to the oncoprotein, Biochemistry 46 (2007) 10405–10412, https://doi.org/10.1021/bi7007917.

[8] B. Todorovic, P. Massimi, K. Hung, G.S. Shaw, L. Banks, J.S. Mymryk, Systematic analysis of the amino acid residues of human papillomavirus type 16 E7 conserved region 3 involved in dimerization and transformation, J. Virol. 85 (2011) 10048–10057, https://doi.org/10.1128/JVI.00643-11.

[9] O. Ohlenschläger, T. Seiboth, H. Zengerling, L. Briese, A. Marchanka, R. Ramachandran, M. Baum, M. Korbas, W. Meyer-Klaucke, M. Dürst, M. Görlach, Solution structure of the partially folded high-risk human papilloma virus 45 oncoprotein E7, Oncogene 25 (2006) 5953–5959, https://doi.org/10.1038/sj.onc.1209584.

[10] J.O. Funk, S. Waga, J.B. Harry, E. Espling, B. Stillman, D.A. Galloway, Inhibition of CDK activity and PCNA-dependent DNA replication by p21 is blocked by interaction with the HPV-16 E7 oncoprotein, Genes Dev. 11 (1997) 2090–2100, https://doi.org/10.1101/gad.11.16.2090.

[11] X. Liu, A. Clements, K. Zhao, R. Marmorstein, Structure of the human Papillomavirus E7 oncoprotein and its mechanism for inactivation of the retinoblastoma tumor suppressor, J. Biol. Chem. 281 (2006) 578–586, https://doi.org/10.1074/jbc.M508455200.

[12] S.L. Gonzalez, M. Stremlau, X. He, J.R. Basile, K. Münger, Degradation of the retinoblastoma tumor suppressor by the human papillomavirus type 16 E7 oncoprotein is important for functional inactivation and is separable from proteasomal degradation of E7, J. Virol. 75 (2001) 7583–7591, https://doi.org/10.1128/JVI.75.16.7583-7591.2001.

[13] C.W. Menges, L.A. Baglia, R. Lapoint, D.J. McCance, Human papillomavirus type 16 E7 up-regulates AKT activity through the retinoblastoma protein, Cancer Res. 66 (2006) 5555–5559, https://doi.org/10.1158/0008-5472.CAN-06-0499.

[14] C. Gui, M. Ji, Y. Song, J. Wang, Y. Zhou, Functions and modulation of PKM2 activity by human papillomavirus E7 oncoprotein (Review), Oncol. Lett. 25 (2023) 7, https://doi.org/10.3892/ol.2022.13593.

[15] E.A. White, K. Münger, P.M. Howley, High-risk human papillomavirus E7 proteins target PTPN14 for degradation, mBio 7 (2016) e01530–16, https://doi.org/10.1128/mBio.01530-16.

[16] A.J. Barr, J.E. Debreczeni, J. Eswaran, S. Knapp, Crystal structure of human protein tyrosine phosphatase 14 (PTPN14) at 1.65-A resolution, Proteins 63 (2006) 1132–1136, https://doi.org/10.1002/prot.20958.

[17] X. Liu, N. Yang, S.A. Figel, K.E. Wilson, C.D. Morrison, I.H. Gelman, J. Zhang, PTPN14 interacts with and negatively regulates the oncogenic function of YAP, Oncogene 32 (2013) 1266–1273, https://doi.org/10.1038/onc.2012.147.

[18] S. Piccolo, S. Dupont, M. Cordenonsi, The biology of YAP/TAZ: hippo signaling and beyond, Physiol. Rev. 94 (2014) 1287–1312, https://doi.org/10.1152/physrev.00005.2014.

[19] C. Michaloglou, W. Lehmann, T. Martin, C. Delaunay, A. Hueber, L. Barys, H. Niu, E. Billy, M. Wartmann, M. Ito, C.J. Wilson, M.E. Digan, A. Bauer, H. Voshol, G. Christofori, W.R. Sellers, F. Hofmann, T. Schmelzle, The tyrosine phosphatase PTPN14 is a negative regulator of YAP activity, PLoS One 8 (2013), e61916, https://doi.org/10.1371/journal.pone.0061916.

[20] K.E. Wilson, N. Yang, A.L. Mussell, J. Zhang, The regulatory role of KIBRA and PTPN14 in hippo signaling and beyond, Genes 7 (2016) 23, https://doi.org/10.3390/genes7060023.

[21] K.E. Wilson, Y.-W. Li, N. Yang, H. Shen, A.R. Orillion, J. Zhang, PTPN14 forms a complex with Kibra and LATS1 proteins and negatively regulates the YAP oncogenic function, J. Biol. Chem. 289 (2014) 23693–23700, https://doi.org/10.1074/jbc.M113.534701.

[22] A. Szalmás, V. Tomaić, O. Basukala, P. Massimi, S. Mittal, J. Kónya, L. Banks, The PTPN14 tumor suppressor is a degradation target of human papillomavirus E7, J. Virol. 91 (2017), e00057-17, https://doi.org/10.1128/JVI.00057-17.

[23] J. Hatterschide, A.E. Bohidar, M. Grace, T.J. Nulton, H.W. Kim, B. Windle, I. M. Morgan, K. Munger, E.A. White, PTPN14 degradation by high-risk human papillomavirus E7 limits keratinocyte differentiation and contributes to HPV-mediated oncogenesis, Proc. Natl. Acad. Sci. U. S. A. 116 (2019) 7033–7042, https://doi.org/10.1073/pnas.1819531116.

[24] H.-Y. Yun, M.W. Kim, H.S. Lee, W. Kim, J.H. Shin, H. Kim, H.-C. Shin, H. Park, B.-H. Oh, W.K. Kim, K.-H. Bae, S.C. Lee, E.-W. Lee, B. Ku, S.J. Kim, Structural basis for recognition of the tumor suppressor protein PTPN14 by the oncoprotein E7 of human papillomavirus, PLoS Biol. 17 (2019), e3000367, https://doi.org/10.1371/journal.pbio.3000367.

[25] V. Salmaso, M. Sturlese, A. Cuzzolin, S. Moro, Combining self- and cross-docking as benchmark tools: the performance of DockBench in the D3R Grand Challenge 2, J. Comput. Aided Mol. Des. 32 (2018) 251–264, https://doi.org/10.1007/s10822-017-0051-4.

[26] O. Korb, T. Stützle, T.E. Exner, Empirical scoring functions for advanced protein-ligand docking with PLANTS, J. Chem. Inf. Model. 49 (2009) 84–96, https://doi.org/10.1021/ci800298z.

[27] M. Celegato, L. Messa, L. Goracci, B. Mercorelli, C. Bertagnin, F. Spyrakis, I. Suarez, A. Cousido-Siah, G. Travé, L. Banks, G. Cruciani, G. Palù, A. Loregian, A novel small-molecule inhibitor of the human papillomavirus E6-p53 interaction that reactivates p53 function and blocks cancer cells growth, Cancer Lett. 470 (2020) 115–125, https://doi.org/10.1016/j.canlet.2019.10.046.

[28] M. Celegato, L. Messa, C. Bertagnin, B. Mercorelli, A. Loregian, Targeted disruption of E6/p53 binding exerts broad activity and synergism with paclitaxel and topotecan against HPV-transformed cancer cells, Cancers 14 (2022) 193, https://doi.org/10.3390/cancers14010193.

[29] G. Nannetti, S. Massari, B. Mercorelli, C. Bertagnin, J. Desantis, G. Palù, O. Tabarrini, A. Loregian, Potent and broad-spectrum cycloheptathiophene-3-carboxamide compounds that target the PA-PB1 interaction of influenza virus RNA polymerase and possess a high barrier to drug resistance, Antivir. Res. 165 (2019) 55–64, https://doi.org/10.1016/j.antiviral.2019.03.003.

[30] G. Muratore, L. Goracci, B. Mercorelli, Á. Foeglein, P. Digard, G. Cruciani, G. Palù, A. Loregian, Small molecule inhibitors of influenza A and B viruses that act by disrupting subunit interactions of the viral polymerase, Proc. Natl. Acad. Sci. U. S. A. 109 (2012) 6247–6252, https://doi.org/10.1073/pnas.1119817109.

[31] L. Messa, M. Celegato, C. Bertagnin, B. Mercorelli, G. Alvisi, L. Banks, G. Palù, A. Loregian, The dimeric form of HPV16 E6 is crucial to drive YAP/TAZ upregulation through the targeting of hScrib, Cancers 13 (2021) 4083, https://doi.org/10.3390/cancers13164083.

[32] L. Messa, M. Celegato, C. Bertagnin, B. Mercorelli, G. Nannetti, G. Palù, A. Loregian, A quantitative LumiFluo assay to test inhibitory compounds blocking p53 degradation induced by human papillomavirus oncoprotein E6 in living cells, Sci. Rep. 8 (2018) 6020, https://doi.org/10.1038/s41598-018-24470-4.

[33] S. Moro, F. Deflorian, M. Bacilieri, G. Spalluto, Ligand-based homology modeling as attractive tool to inspect GPCR structural plasticity, Curr. Pharmaceut. Des. 12 (2006) 2175–2185, https://doi.org/10.2174/138161206777585265.

[34] J. Desantis, G. Nannetti, S. Massari, M.L. Barreca, G. Manfroni, V. Cecchetti, G. Palù, L. Goracci, A. Loregian, O. Tabarrini, Exploring the cycloheptathiophene-3-carboxamide scaffold to disrupt the interactions of the influenza polymerase subunits and obtain potent anti-influenza activity, Eur. J. Med. Chem. 138 (2017) 128–139, https://doi.org/10.1016/j.ejmech.2017.06.015.

[35] D. Trisciuzzi, O. Nicolotti, M.A. Miteva, B.O. Villoutreix, Analysis of solvent-exposed and buried co-crystallized ligands: a case study to support the design of novel protein-protein interaction inhibitors, Drug Discov. Today 24 (2019) 551–559, https://doi.org/10.1016/j.drudis.2018.11.013.

[36] D. Martinez-Zapien, F.X. Ruiz, J. Poirson, A. Mitschler, J. Ramirez, A. Forster, A. Cousido-Siah, M. Masson, S. Vande Pol, A. Podjarny, G. Travé, K. Zanier, Structure of the E6/E6AP/p53 complex required for HPV-mediated degradation of p53, Nature 529 (2016) 541–545, https://doi.org/10.1038/nature16481.

[37] S.S. Mello, L.J. Valente, N. Raj, J.A. Seoane, B.M. Flowers, J. McClendon, K. T. Bieging-Rolett, J. Lee, D. Ivanochko, M.M. Kozak, D.T. Chang, T.A. Longacre, A. C. Koong, C.H. Arrowsmith, S.K. Kim, H. Vogel, L.D. Wood, R.H. Hruban, C. Curtis, L.D. Attardi, A p53 super-tumor suppressor reveals a tumor suppressive p53-ptpn14-yap Axis in pancreatic cancer, Cancer Cell 32 (2017) 460–473, https://doi.org/10.1016/j.ccell.2017.09.007.

[38] J.O. Lee, A.A. Russo, N.P. Pavletich, Structure of the retinoblastoma tumour-suppressor pocket domain bound to a peptide from HPV E7, Nature 391 (1998) 859–865, https://doi.org/10.1038/36038.

[39] Y. Liu-Chittenden, B. Huang, J.S. Shim, Q. Chen, S.-J. Lee, R.A. Anders, J.O. Liu, D. Pan, Genetic and pharmacological disruption of the TEAD-YAP complex suppresses the oncogenic activity of YAP, Genes Dev. 26 (2012) 1300–1305, https://doi.org/10.1101/gad.192856.112.

[40] J. Feng, J. Gou, J. Jia, T. Yi, T. Cui, Z. Li, Verteporfin, a suppressor of YAP-TEAD complex, presents promising antitumor properties on ovarian cancer, OncoTargets Ther. 9 (2016) 5371–5381, https://doi.org/10.2147/OTT.S109979.

[41] J. Wei, J. Yao, C. Yang, Y. Mao, D. Zhu, Y. Xie, P. Liu, M. Yan, L. Ren, Y. Lin, Q. Zheng, X. Li, Heterogeneous matrix stiffness regulates the cancer stem-like cell phenotype in hepatocellular carcinoma, J. Transl. Med. 20 (2022) 555, https://doi.org/10.1186/s12967-022-03778-w.

[42] J. Luo, H. Zou, Y. Guo, T. Tong, Y. Chen, Y. Xiao, Y. Pan, P. Li, The oncogenic roles and clinical implications of YAP/TAZ in breast cancer, Br. J. Cancer 128 (2023) 1611–1624, https://doi.org/10.1038/s41416-023-02182-5.

[43] T.B. Steinbichler, J. Dudás, S. Skvortsov, U. Ganswindt, H. Riechelmann, I.-I. Skvortsova, Therapy resistance mediated by cancer stem cells, Semin. Cancer Biol. 53 (2018) 156–167, https://doi.org/10.1016/j.semcancer.2018.11.006.

[44] L. Messa, A. Loregian, HPV-induced cancers: preclinical therapeutic advancements, Expert Opin. Invest. Drugs 31 (2022) 79–93, https://doi.org/10.1080/13543784.2021.2010703.

[45] S.F. Jabbar, L. Abrams, A. Glick, P.F. Lambert, Persistence of high-grade cervical dysplasia and cervical cancer requires the continuous expression of the human papillomavirus type 16 E7 oncogene, Cancer Res. 69 (2009) 4407–4414, https://doi.org/10.1158/0008-5472.CAN-09-0023.

[46] S.F. Jabbar, S. Park, J. Schweizer, M. Berard-Bergery, H.C. Pitot, D. Lee, P. F. Lambert, Cervical cancers require the continuous expression of the human papillomavirus type 16 E7 oncoprotein even in the presence of the viral E6 oncoprotein, Cancer Res. 72 (2012) 4008–4016, https://doi.org/10.1158/0008-5472.CAN-11-3085.

[47] R. Herber, A. Liem, H. Pitot, P.F. Lambert, Squamous epithelial hyperplasia and carcinoma in mice transgenic for the human papillomavirus type 16 E7 oncogene, J. Virol. 70 (1996) 1873–1881, https://doi.org/10.1128/JVI.70.3.1873-1881.1996.

[48] R.R. Riley, S. Duensing, T. Brake, K. Münger, P.F. Lambert, J.M. Arbeit, Dissection of human papillomavirus E6 and E7 function in transgenic mouse models of cervical carcinogenesis, Cancer Res. 63 (2003) 4862–4871.

[49] S. Balsitis, F. Dick, N. Dyson, P.F. Lambert, Critical roles for non-pRb targets of human papillomavirus type 16 E7 in cervical carcinogenesis, Cancer Res. 66 (2006) 9393–9400, https://doi.org/10.1158/0008-5472.CAN-06-0984.

[50] G.A. Gulliver, R.L. Herber, A. Liem, P.F. Lambert, Both conserved region 1 (CR1) and CR2 of the human papillomavirus type 16 E7 oncogene are required for induction of epidermal hyperplasia and tumor formation in transgenic mice, J. Virol. 71 (1997) 5905–5914, https://doi.org/10.1128/JVI.71.8.5905-5914.1997.

[51] J. Hatterschide, A.C. Brantly, M. Grace, K. Munger, E.A. White, A conserved amino acid in the C terminus of human papillomavirus E7 mediates binding to PTPN14 and repression of epithelial differentiation, J. Virol. 94 (2020), e01024-20, https://doi.org/10.1128/JVI.01024-20.

[52] F. Zanconato, M. Cordenonsi, S. Piccolo, YAP/TAZ at the roots of cancer, Cancer Cell 29 (2016) 783–803, https://doi.org/10.1016/j.ccell.2016.05.005.

[53] J.H. Park, J.E. Shin, H.W. Park, The role of Hippo pathway in cancer stem cell biology, Mol. Cells 41 (2018) 83–92, https://doi.org/10.14348/molcells.2018.2242.

[54] R. Abylkassov, Y. Xie, Role of Yes-associated protein in cancer: an update, Oncol. Lett. 12 (2016) 2277–2282, https://doi.org/10.3892/ol.2016.4955.

[55] D. Fera, D.C. Schultz, S. Hodawadekar, M. Reichman, P.S. Donover, J. Melvin, S. Troutman, J.L. Kissil, D.M. Huryn, R. Marmorstein, Identification and characterization of small molecule antagonists of pRb inactivation by viral oncoproteins, Chem. Biol. 19 (2012) 518–528, https://doi.org/10.1016/j.chembiol.2012.03.007.

[56] M. Aarthy, S.K. Singh, Interpretations on the interaction between protein tyrosine phosphatase and E7 oncoproteins of high and low-risk HPV: a computational perception, ACS Omega 6 (2021) 16472–16487, https://doi.org/10.1021/acsomega.1c01619.

[57] A.J. Souers, J.D. Leverson, E.R. Boghaert, S.L. Ackler, N.D. Catron, J. Chen, B. D. Dayton, H. Ding, S.H. Enschede, W.J. Fairbrother, D.C. Huang, S.G. Hymowitz, S. Jin, S.L. Khaw, P.J. Kovar, L.T. Lam, J. Lee, H.L. Maecker, K.C. Marsh, K. D. Mason, M.J. Mitten, P.M. Nimmer, A. Oleksijew, C.H. Park, C.M. Park, D. C. Phillips, A.W. Roberts, D. Sampath, J.F. Seymour, M.L. Smith, G.M. Sullivan, S. K. Tahir, C. Tse, M.D. Wendt, Y. Xiao, J.C. Xue, H. Zhang, R.A. Humerickhouse, S. H. Rosenberg, S.W. Elmore, ABT-199, a potent and selective BCL-2 inhibitor, achieves antitumor activity while sparing platelets, Nat. Med. 19 (2013) 202–208, https://doi.org/10.1038/nm.3048.

[58] W. Xiang, L. Zhao, X. Han, C. Qin, B. Miao, D. McEachern, Y. Wang, H. Metwally, P. D. Kirchhoff, L. Wang, A. Matvekas, M. He, B. Wen, D. Sun, S. Wang, Discovery of ARD-2585 as an exceptionally potent and orally active PROTAC degrader of androgen receptor for the treatment of advanced prostate cancer, J. Med. Chem. 64 (2021) 13487–13509, https://doi.org/10.1021/acs.jmedchem.1c00900.

[59] X. Jia, X. Han, Targeting androgen receptor degradation with PROTACs from bench to bedside, Biomed. Pharmacother. 158 (2023), 114112, https://doi.org/10.1016/j.biopha.2022.114112.

[60] Y. Xue, A.A. Bolinger, J. Zhou, Novel approaches to targeted protein degradation technologies in drug discovery, Expert Opin. Drug Discov. 18 (2023) 467–483, https://doi.org/10.1080/17460441.2023.2187777.